

Chiral supersymmetric models on an orientifold of $\mathbb{Z}_4 \times \mathbb{Z}_2$ with intersecting D6-branes

Gabriele Honecker

*Departamento de Física Teórica C-XI and Instituto de Física Teórica C-XVI,
Universidad Autónoma de Madrid, Cantoblanco, 28049 Madrid, Spain*

Abstract

We investigate intersecting D6-branes on an orientifold of type IIA theory in the orbifold background $T^6/(\mathbb{Z}_4 \times \mathbb{Z}_2)$ with the emphasis on finding chiral spectra. RR tadpole cancellation conditions and the scalar potential at disc level are computed. The general chiral spectrum is displayed, and two supersymmetric models with a Pati-Salam group are shown, one with four generations and the other one with three generations and *exactly* the chiral matter content of the SM plus right handed neutrinos.

1 Introduction

In the recent years, open string models have started to play a key role in constructing phenomenologically appealing string vacua as well as getting a deeper understanding of the still unknown M-theory. The two major approaches in this direction consist in constructing chiral theories from D-brane set-ups in type II orientifold theories. One possibility relies on D-branes located at singularities which support chiral fermions on their worldvolume, see e.g. [1, 2]. In the other approach, D-branes wrap some compact dimensions, and chiral fermions are located at intersections of D-branes [3] wrapping different compact cycles. The search for chiral and stable vacua in this framework has turned out to be highly non-trivial. The first models with D-branes intersecting at angles were those where the D-branes are located on top of orientifold planes also at angles in an orbifold background. All these models turned out to be supersymmetric but non-chiral [4, 5]. Subsequently, general features for model building within intersecting brane world scenarios, e.g. family replication as well as the leading order behavior of gauge and Yukawa couplings in terms of geometric quantities of the compactification, were worked out in [6, 7, 8].

The picture of D-branes at non-trivial angles has a T-dual formulation in terms of D-branes with different magnetic background fluxes. An early observation on the possibility of supersymmetry breaking in this language was made in [9]. Further works in the picture with background fluxes were performed in [10].

Pioneered by [11], searches for exact realizations of the standard model and GUT models from intersecting D6-branes were performed in a number of papers [12, 13], and phenomenological issues for these models, e.g. the appearance of additional $U(1)$ symmetries and the interpretation of the Higgs mechanism as brane recombination, were addressed in more detail [14]; for a very recent discussion on the exact structure of Yukawa couplings see also [15].

Motivated by large extra dimension scenarios [16], models with intersecting D4- and D5-branes with and without orientifold projections in the type II string theory framework were as well investigated in [17]. A related model within the type 0' theory was discussed in [18], and applications to cosmology started to be considered (see e.g. [19]).

In [20], generalizations of intersecting D-brane set-ups beyond the conformal field theory limit on orbifolds were discussed.

In general, the chiral models are non-supersymmetric. Even if the low energy spectra are free of tachyons, NSNS tadpoles signal that the analysis is performed in a false vacuum. Furthermore, D6-branes at angles do not allow for large extra dimensions but enforce the string scale to be of the order of the Planck scale.

These problems do, however, not apply to supersymmetric models. In [21], a class of chiral supersymmetric models with intersecting D6-branes in the orbifold background $T^6/(\mathbb{Z}_2 \times \mathbb{Z}_2)$ was constructed. The phenomenology for standard model like spectra was subsequently worked out in [22]. A systematic search for $SU(5)$ GUT models has also been performed recently [23].

Together with the T^6/\mathbb{Z}_4 orientifold model in [24], these are the two only known cases of models with D6-branes intersecting at angles which preserve supersymmetry and provide phenomenologically appealing chiral spectra but, however, contain some exotic matter.

Last but not least, another motivation to proceed with the search for chiral supersymmetric vacua from intersecting D6-branes consists in the fact that only the supersymmetric case lifts to a purely geometrical background in M-theory on a manifold with G_2 holonomy (see e.g. [25] and the corresponding sections in [21, 20] plus references therein).

In this paper, we search for chiral supersymmetric models in a type IIA orientifold on $T^6/(\mathbb{Z}_4 \times \mathbb{Z}_2)$. The most simple non-chiral model on this orbifold was already found in [5]. Many features are similar to the simpler chiral model with product orbifold group $T^6/(\mathbb{Z}_2 \times \mathbb{Z}_2)$ [21], but as in the case of T^6/\mathbb{Z}_4 [24], the D6-branes lie in certain invariant orbits under the orbifold group which make the analysis more involved.

The paper is organized as follows: in section 2, the geometry of the compactification on $T^6/(\mathbb{Z}_4 \times \mathbb{Z}_2)$ and basic model building ingredients are described. In section 3, details of the RR tadpole cancellation calculation and the required D6-brane configuration are given. Subsequently, in section 4 the chiral spectrum is displayed. NSNS tadpoles are briefly commented on in section 5. Two chiral models with a Pati - Salam gauge group — including one with three generations and no exotic chiral matter — are discussed in section 6. Finally, the conclusions are given in section 7 and some further technical details of the calculation are collected in two appendices A and B.

2 Geometry of the $T^6/(\Omega\mathcal{R} \times \mathbb{Z}_4 \times \mathbb{Z}_2)$ orientifold

Throughout the paper, we consider an orientifold of type IIA string theory compactified on the orbifold $T^6/(\mathbb{Z}_4 \times \mathbb{Z}_2)$. The orbifold group $\mathbb{Z}_4 \times \mathbb{Z}_2$ is generated by

$$\begin{aligned}\Theta : & \quad (z^1, z^2, z^3) \rightarrow (iz^1, -iz^2, z^3), \\ \omega : & \quad (z^1, z^2, z^3) \rightarrow (z^1, -z^2, -z^3),\end{aligned}$$

where $z^1 = x^4 + ix^5$, $z^2 = x^6 + ix^7$, $z^3 = x^8 + ix^9$ label the internal complex coordinates of the six-torus which we consider to be decomposed into a product of three two-tori, $T^6 \simeq T_1^2 \times T_2^2 \times T_3^2$. This orbifold group action describes the singular limit of a Calabi-Yau compactification preserving $\mathcal{N} = 2$ supersymmetry in four dimensions. The Hodge numbers of this manifold are $h_{1,1} = 61$ and $h_{2,1} = 1$.¹ The number of independent 3-cycles is given by $b_3 = 2 + 2h_{2,1} = 4$, which means that all 3-cycles of this model are inherited from the six-torus T^6 . This is in contrast to the T^6/\mathbb{Z}_4 orbifold which was considered in [24] where also exceptional cycles have to be included in the analysis of the underlying geometry. Furthermore, three $(1, 1)$ -forms are inherited from the torus, and $18 + 12 + 12$ arise from fixtori under Θ^2, ω and $\Theta^2\omega$, respectively. The fixedpoints of $\Theta\omega$ provide 16 further $(1, 1)$ -forms.

In addition to the orbifold group, we perform an orientifold projection $\Omega\mathcal{R}$ which was first employed in [4, 5]. The worldsheet parity Ω is accompanied by a geometric action on the compact space,

$$\mathcal{R} : \quad z^i \longrightarrow z^{\bar{i}}, \quad i = 1, 2, 3.$$

This projection introduces O6-planes which are located at the 3-cycles invariant under $\mathcal{R}\Theta^k\omega^l$ for $k = 0, \dots, 3$ and $l = 0, 1$. In order to cancel the RR tadpoles which arise from the O6-planes, one is forced to include D6-branes intersecting at angles in the model. An explicit NSNS three-form flux H_{NS} might also play a role in canceling chiral anomalies [26], which, however, is not taken into account in this paper since the search here is focused on supersymmetric models. In the most simple example of this kind, the D6-branes lie on top of the O6-planes and cancel all RR-charges locally leading to a purely non-chiral spectrum as investigated in [5].

¹I am grateful to K. Wendland for the computation of the Hodge numbers. See also [2].

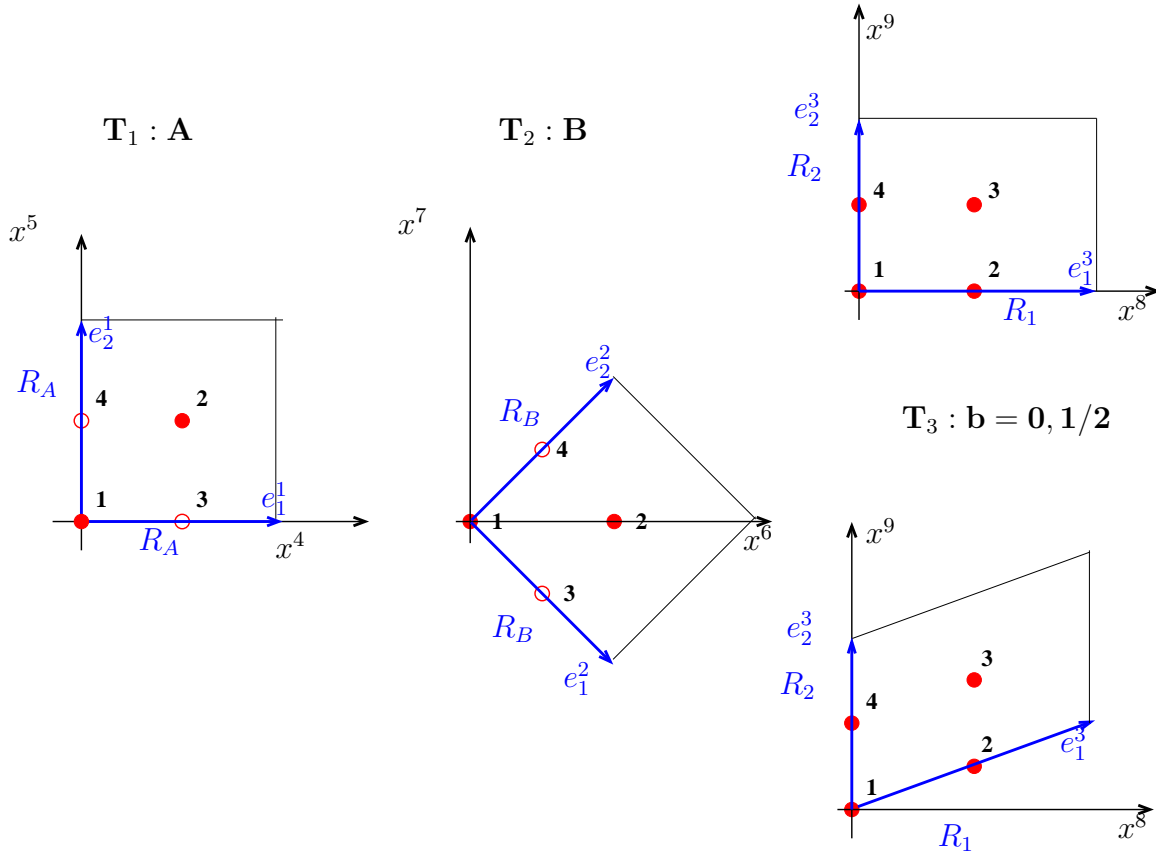


Figure 1: The possible choices of the compactification lattices per two-torus. \mathbb{Z}_4 fixed points are depicted by filled circles, the additional points invariant under \mathbb{Z}_2 subsymmetries by empty circles. The basis of each two-torus in our convention is displayed in blue. The two possible choices of the third lattice correspond to a vanishing and non-trivial antisymmetric tensor background on \tilde{T}_3^2 in the T-dual type IIB orientifold, respectively.

The constraints on the shape of the two-tori imposed by the orbifold group $\mathbb{Z}_4 \times \mathbb{Z}_2$ and the anti-holomorphic involution \mathcal{R} are the same as for the \mathbb{Z}_4 model considered in [24]. Namely, the complex structure moduli on the first two tori $T_1^2 \times T_2^2$ are fixed by the \mathbb{Z}_4 symmetry such as to parameterize square tori. Furthermore, the reflexion \mathcal{R} enforces the orientation of the lattices to be either of type **A** or **B** as depicted in figure 1. The radii R_A and R_B remain as moduli of the compactification. The third torus T_3^2 is not constrained by the orbifold action since it is only subject to a \mathbb{Z}_2 rotation. The reflexion \mathcal{R} , however, constrains its shape. The two allowed choices correspond in the T-dual type IIB orientifold model, where T-duality is taken to act along the x^9 coordinate, to the possibility of having either a vanishing or a non-trivial quantized antisymmetric tensor background on the dual torus \tilde{T}_3^2 conveniently parameterized by $b = 0, 1/2$, respectively [7]. In addition, the imaginary part of the complex structure and the volume are moduli which can be parameterized by the two radii R_1 and R_2 as depicted in figure 1.

The factorizable 3-cycles which the $O6_a$ -planes and $D6_a$ -branes wrap are conveniently characterized by the wrapping numbers (n_i^a, m_i^a) on the i^{th} two-torus T_i^2 along the basis (e_1^i, e_2^i) displayed in figure 1. In general, different kinds of $D6$ -branes a and b intersect several times on

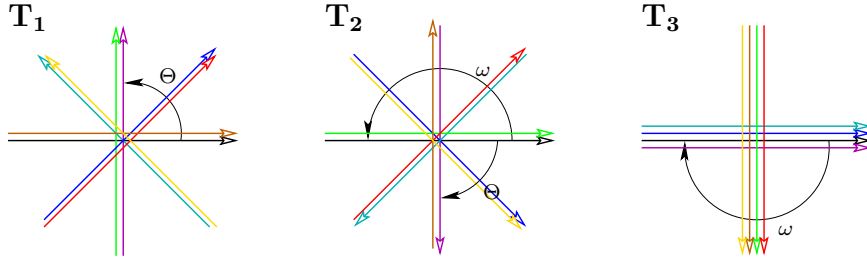


Figure 2: The four orbits of O6-planes. Each orbit consists of an O6-plane and its image under the \mathbb{Z}_4 generator Θ . The black and the purple cycles belong to one orbit, the red and the yellow cycles form another orbit. The remaining orbits consist of the blue and cyan cycles and the green and brown ones.

the fundamental cell of the torus. The intersection number in terms of wrapping numbers is given by

$$I_{ab} = \prod_{i=1,2,3} (n_i^a m_i^b - n_i^b m_i^a).$$

The symmetries \mathcal{R} and Θ enforce the positions of O6-planes and D6-branes to be grouped into invariant orbits as described in more detail in section 3 in the course of calculating the Klein bottle and Möbius strip amplitudes.

3 RR tadpole cancellation

The requirement of vanishing net RR-charge constrains the allowed sets of wrapping numbers and numbers of identical D6-branes. The values depend on the shape of the third torus or, in the T-dual picture, on the value of the antisymmetric tensor background.

The Klein bottle amplitude

The Klein bottle amplitude can be easily obtained from the computation in [5] where the calculation had been constrained to the case $R_2 = 4^b R_1$ which parameterizes a square torus T_3^2 with orientation **A** or **B** for $b = 0, 1/2$, respectively. There exist in total three inequivalent choices of complex structures on $T_1^2 \times T_2^2$, namely **AA**, **AB** and **BB**. As in [5], we only consider the case where the lattice on $T_1^2 \times T_2^2$ is chosen to be of the kind **AB** since, only in this case, the worldsheet duality is well understood in terms of introducing one sort of boundary and crosscap states.

The eight kinds of O6-planes required by the $\Omega\mathcal{R} \times \mathbb{Z}_4 \times \mathbb{Z}_2$ symmetry are displayed in figure 2. They are grouped into four orbits of two kinds of O6-planes each which are mapped onto each other under the \mathbb{Z}_4 generator Θ . The O6-planes wrapping the x^8 direction contribute a constant times R_1/R_2 to the tadpoles due to the windings perpendicular and momenta parallel to its position. In the same spirit, the contribution originating from the O6-planes wrapping the x^9 direction are proportional to R_2/R_1 .

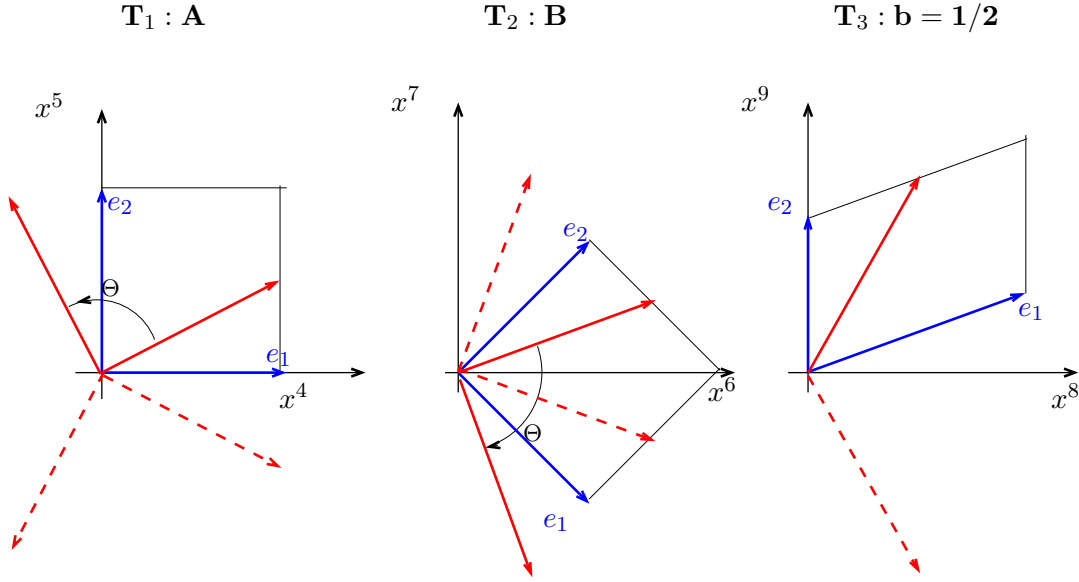


Figure 3: Orbit of a D6-brane with wrapping numbers $(n_1^a, m_1^a) = (2, 1)$, $(n_2^a, m_2^a) = (1, 2)$, $(n_3^a, m_3^a) = (1, 2)$ on a tilted torus T_3^2 , i.e. $b = 1/2$. The brane a and its \mathbb{Z}_4 image (Θa) are represented by solid red lines whereas the mirror images a' and $(\Theta a)'$ are depicted by dashed red lines.

The resulting tadpole of the Klein bottle amplitude in the tree channel is given by

$$\mathcal{K} \rightarrow (1_{RR} - 1_{NSNS})2^9 c \left(\frac{R_1}{R_2} + \frac{1}{16^b} \frac{R_2}{R_1} \right) \int_0^\infty dl. \quad (1)$$

The Möbius strip amplitude

The general orbit of a D6-brane consists of four different cycles. A brane a is mapped under the \mathbb{Z}_4 rotation to its image (Θa) and under \mathcal{R} these two are mapped onto their mirror images a' and $(\Theta a)'$. The wrapping numbers of such an orbit are given by

$$a \Leftrightarrow \begin{pmatrix} n_1^a & m_1^a \\ n_2^a & m_2^a \\ n_3^a & m_3^a \end{pmatrix}, \quad (\Theta a) \Leftrightarrow \begin{pmatrix} -m_1^a & n_1^a \\ m_2^a & -n_2^a \\ n_3^a & m_3^a \end{pmatrix},$$

$$a' \Leftrightarrow \begin{pmatrix} n_1^a & -m_1^a \\ m_2^a & n_2^a \\ n_3^a & -m_3^a - 2bn_3^a \end{pmatrix}, \quad (\Theta a)' \Leftrightarrow \begin{pmatrix} -m_1^a & -n_1^a \\ -n_2^a & m_2^a \\ n_3^a & -m_3^a - 2bn_3^a \end{pmatrix}.$$

An example of a whole D6-brane orbit is depicted in figure 3.

The Möbius strip amplitude has contributions from two different kinds of strings: the aa' strings — which are identified with the $(\Theta a)(\Theta a)'$ strings via a \mathbb{Z}_4 rotation — are invariant under $\Omega\mathcal{R}\Theta^{2k}\omega^l$. The $a(\Theta a)'$ strings and their rotated images $(\Theta a)a'$ correspond to ‘twisted open strings’ in the language of [5] and are invariant under $\Omega\mathcal{R}\Theta^{2k+1}\omega^l$.

The loop channel expression for the aa' strings is given by

$$\begin{aligned} \mathcal{M}_{aa'} &= \frac{c}{2^5} \sum_{k,l=0}^1 i(-1)^{l+1} e^{2i \sum_{j=1}^3 \delta_j^{(k,l)} \varphi_j} \text{tr} \left(\gamma_{\Omega \mathcal{R} \Theta^{2k} \omega^l}^{-T,a'} \gamma_{\Omega \mathcal{R} \Theta^{2k} \omega^l}^a \right) I_{aa'}^{\Omega \mathcal{R} \Theta^{2k} \omega^l} \\ &\quad \times \int_0^\infty \frac{dt}{t^3} \frac{\vartheta \left[\begin{smallmatrix} \frac{1}{2} \\ 0 \end{smallmatrix} \right]}{\eta^3} \prod_{j=1}^3 \frac{\vartheta \left[\begin{smallmatrix} \frac{1}{2} + 2 \frac{\varphi_j}{\pi} \\ \frac{1 - \delta_j^{(k,l)}}{4} - \frac{\varphi_j}{\pi} \end{smallmatrix} \right]}{\vartheta \left[\begin{smallmatrix} \frac{1}{2} + 2 \frac{\varphi_j}{\pi} \\ \frac{1 + \delta_j^{(k,l)}}{4} - \frac{\varphi_j}{\pi} \end{smallmatrix} \right]} \left(t - \frac{i}{2} \right) \end{aligned}$$

with the phases $\delta_1^{(k,l)} = (-1)^k$, $\delta_2^{(k,l)} = (-1)^{k+l}$ and $\delta_3^{(k,l)} = (-1)^l$. $I_{aa'}^{\Omega \mathcal{R} \Theta^{2k} \omega^l}$ denotes the numbers of intersections between the branes a and a' which are invariant under $\mathcal{R} \Theta^{2k} \omega^l$ and φ_j is the angle of brane a with respect to the \mathcal{R} invariant axis on the j^{th} two-torus T_j^2 . Performing the modular transformation $t = \frac{1}{sl}$ yields the tree channel expression of the amplitude,

$$\mathcal{M}_{aa'} = -\frac{c}{2} \sum_{k,l=0}^1 (-1)^l \text{tr} \left(\gamma_{\Omega \mathcal{R} \Theta^{2k} \omega^l}^{-T,a'} \gamma_{\Omega \mathcal{R} \Theta^{2k} \omega^l}^a \right) I_{aa'}^{\Omega \mathcal{R} \Theta^{2k} \omega^l} \int_0^\infty dl \frac{\vartheta \left[\begin{smallmatrix} \frac{1}{2} \\ 0 \end{smallmatrix} \right]}{\eta^3} \prod_{j=1}^3 \frac{\vartheta \left[\begin{smallmatrix} \frac{1}{2} \\ \frac{1 - \delta_j^{(k,l)}}{4} + \frac{\varphi_j}{\pi} \end{smallmatrix} \right]}{\vartheta \left[\begin{smallmatrix} \frac{1}{2} \\ \frac{1 + \delta_j^{(k,l)}}{4} + \frac{\varphi_j}{\pi} \end{smallmatrix} \right]} \left(2l - \frac{i}{2} \right). \quad (2)$$

The contribution to the Möbius strip amplitude originating from the $a(\Theta a)'$ strings is computed along the same lines. The loop channel expression is given by

$$\begin{aligned} \mathcal{M}_{a(\Theta a)'} &= \frac{c}{2^5} \sum_{k,l=0}^1 i(-1)^{l+1} e^{2i \sum_{j=1}^3 \epsilon_j^{(k,l)} \varphi_j} I_{a(\Theta a)'}^{\Omega \mathcal{R} \Theta^{2k+1} \omega^l} \text{tr} \left(\gamma_{\Omega \mathcal{R} \Theta^{2k+1} \omega^l}^{-T,(\Theta a)'} \gamma_{\Omega \mathcal{R} \Theta^{2k+1} \omega^l}^a \right) \\ &\quad \times \int_0^\infty \frac{dt}{t^3} \frac{\vartheta \left[\begin{smallmatrix} \frac{1}{2} \\ 0 \end{smallmatrix} \right]}{\eta^3} \left(\prod_{j=1}^2 \frac{\vartheta \left[\begin{smallmatrix} \frac{2\varphi_j}{\pi} \\ \frac{\epsilon_j^{(k,l)}}{4} - \frac{\varphi_j}{\pi} \end{smallmatrix} \right]}{\vartheta \left[\begin{smallmatrix} \frac{2\varphi_j}{\pi} \\ \frac{\epsilon_j^{(k,l)}}{4} - \frac{\varphi_j}{\pi} \end{smallmatrix} \right]} \right) \frac{\vartheta \left[\begin{smallmatrix} \frac{1}{2} + 2 \frac{\varphi_3}{\pi} \\ \frac{1 - \epsilon_3^{(k,l)}}{4} - \frac{\varphi_3}{\pi} \end{smallmatrix} \right]}{\vartheta \left[\begin{smallmatrix} \frac{1}{2} + 2 \frac{\varphi_3}{\pi} \\ \frac{1 + \epsilon_3^{(k,l)}}{4} - \frac{\varphi_3}{\pi} \end{smallmatrix} \right]} \left(t - \frac{i}{2} \right) \end{aligned}$$

with the phases $\epsilon_1^{(k,l)} = -(-1)^k$, $\epsilon_2^{(k,l)} = (-1)^{k+l}$ and $\epsilon_3^{(k,l)} = (-1)^l$. Upon modular transformation, one obtains the tree channel expression

$$\begin{aligned} \mathcal{M}_{a(\Theta a)'} &= -\frac{c}{2} \sum_{k,l=0}^1 (-1)^l \text{tr} \left(\gamma_{\Omega \mathcal{R} \Theta^{2k+1} \omega^l}^{-T,(\Theta a)'} \gamma_{\Omega \mathcal{R} \Theta^{2k+1} \omega^l}^a \right) I_{a(\Theta a)'}^{\Omega \mathcal{R} \Theta^{2k+1} \omega^l} \\ &\quad \times \int_0^\infty dl \frac{\vartheta \left[\begin{smallmatrix} \frac{1}{2} \\ 0 \end{smallmatrix} \right]}{\eta^3} \left(\prod_{j=1}^2 \frac{\vartheta \left[\begin{smallmatrix} \frac{1}{2} \\ \frac{\epsilon_j^{(k,l)}}{4} + \frac{\varphi_j}{\pi} \end{smallmatrix} \right]}{\vartheta \left[\begin{smallmatrix} \frac{1}{2} \\ \frac{\epsilon_j^{(k,l)}}{4} + \frac{\varphi_j}{\pi} \end{smallmatrix} \right]} \right) \frac{\vartheta \left[\begin{smallmatrix} \frac{1}{2} \\ \frac{1 - \epsilon_3^{(k,l)}}{4} + \frac{\varphi_3}{\pi} \end{smallmatrix} \right]}{\vartheta \left[\begin{smallmatrix} \frac{1}{2} \\ \frac{1 + \epsilon_3^{(k,l)}}{4} + \frac{\varphi_3}{\pi} \end{smallmatrix} \right]} \left(2l - \frac{i}{2} \right). \quad (3) \end{aligned}$$

Summing over all invariant brane configurations, (2) and (3) lead to the following contribution of the total Möbius strip amplitude to the RR tadpole,

$$\mathcal{M}_{RR} \rightarrow -2^5 c \left(\frac{R_1}{R_2} \sum_a N_a (n_1^a N_2^a + m_1^a M_2^a) n_3^a + \frac{R_2}{R_1} \sum_a N_a (n_1^a M_2^a - m_1^a N_2^a) \frac{M_3^a}{4^b} \right) \int_0^\infty dl, \quad (4)$$

where the following abbreviations for linear combinations of wrapping numbers have been used in order to shorten the formulas

$$\begin{aligned} N_2^a &= n_2^a + m_2^a, \\ M_2^a &= n_2^a - m_2^a, \\ M_3^a &= m_3^a + bn_3^a. \end{aligned} \tag{5}$$

$N_a = \pm \text{tr}(\gamma_{\Omega\mathcal{R}\Theta^k\omega^l}^{-T} \gamma_{\Omega\mathcal{R}\Theta^k\omega^l})$ denotes the number of identical D6-branes. The signs of the traces are chosen such that the sum of RR tadpoles of Klein bottle, Möbius strip and annulus amplitude gives a sum of perfect squares. The actual choice of Chan Paton matrices is listed in section 4, equation (8).

The annulus amplitude

The annulus amplitude is computed in the same way as for the toroidal models studied in [6]. All $\mathbb{Z}_2 \times \mathbb{Z}_2$ insertions $\Theta^{2k}\omega^l$ in the loop channel preserve any configuration of D6-branes but lead to \mathbb{Z}_2 twisted RR charges which cannot be compensated for by the Klein bottle and Möbius strip amplitudes. Therefore, as in the previously studied cases with \mathbb{Z}_2 subsymmetries [4, 5, 7, 21], the prefactors of the amplitudes with $\Theta^{2k}\omega^l$ insertions have to vanish, i.e. $\text{tr}\gamma_{\Theta^{2k}\omega^l} = 0$ for all D6-branes.

Taking into account all contributions to the total annulus amplitude coming from the D6-branes as well as their Θ and \mathcal{R} orbits, the resulting RR tadpole is given by

$$\mathcal{A}_{RR} \rightarrow \frac{1}{2} \left(\frac{R_1}{R_2} \left[\sum_a N_a (n_1^a N_2^a + m_1^a M_2^a) n_3^a \right]^2 + \frac{R_2}{R_1} \left[\sum_a N_a (n_1^a M_2^a - m_1^a N_2^a) M_3^a \right]^2 \right) \int_0^\infty dl. \tag{6}$$

RR tadpole cancellation

The formulas (1), (4) and (6) provide two independent RR tadpole cancellation conditions corresponding to the fact that the two radii R_1 and R_2 of T_3^2 are not constrained by the symmetries of the compactification:

$$\begin{aligned} \sum_a (n_1^a N_2^a + m_1^a M_2^a) n_3^a N_a &= 32, \\ \sum_a (n_1^a M_2^a - m_1^a N_2^a) M_3^a N_a &= \frac{32}{4^b}, \end{aligned} \tag{7}$$

where again $b = 0, 1/2$ corresponds to the two different allowed shapes of T_3^2 and the abbreviations (5) have been used.

This matches by comparison with the supersymmetric non-chiral model in [5] when taking into account that $\Omega\mathcal{R}$ and $\Omega\mathcal{R}\Theta$ invariant D6-branes occur only in orbits of two different cycles (cp. figure 2) instead of four in the generic case and thus contribute only half of the amount of an arbitrary D6-brane to the RR-tadpole cancellation conditions.

4 General open spectrum

Chiral spectrum

The massless closed string spectrum consists of 57 chiral and one vector multiplet for $b = 0$ and of 47 chiral plus eleven vectormultiplets for $b = 1/2$ [5]. A consistent choice of the Chan Paton projection matrices for a and a' simultaneously is provided by

$$\begin{aligned} \gamma_{\Theta}^a &= \begin{pmatrix} e^{i\pi/4} \mathbb{1}_{N_a/2} & 0 & 0 & 0 \\ 0 & e^{-i\pi/4} \mathbb{1}_{N_a/2} & 0 & 0 \\ 0 & 0 & e^{-i\pi/4} \mathbb{1}_{N_a/2} & 0 \\ 0 & 0 & 0 & e^{i\pi/4} \mathbb{1}_{N_a/2} \end{pmatrix}, \\ \gamma_{\omega}^a &= \begin{pmatrix} 0 & \mathbb{1}_{N_a/2} & 0 & 0 \\ -\mathbb{1}_{N_a/2} & 0 & 0 & 0 \\ 0 & 0 & 0 & \mathbb{1}_{N_a/2} \\ 0 & 0 & -\mathbb{1}_{N_a/2} & 0 \end{pmatrix}, \quad \gamma_{\Omega\mathcal{R}}^a = \begin{pmatrix} 0 & 0 & \mathbb{1}_{N_a/2} & 0 \\ 0 & 0 & 0 & \mathbb{1}_{N_a/2} \\ \mathbb{1}_{N_a/2} & 0 & 0 & 0 \\ 0 & \mathbb{1}_{N_a/2} & 0 & 0 \end{pmatrix}. \end{aligned} \quad (8)$$

The matrices are chosen to be of identical shape for all kinds of D6_a-branes. The corresponding Chan Paton matrices for the \mathbb{Z}_4 rotated branes (Θa) are obtained from the consistency conditions in the Möbius strip amplitude calculation $\gamma_{\Omega\mathcal{R}\Theta^{2k+1}\omega^l}^{T,(\Theta a)'} = \pm \gamma_{\Omega\mathcal{R}\Theta^{2k+1}\omega^l}^a$. Note that the $\Omega\mathcal{R} \times \mathbb{Z}_2 \times \mathbb{Z}_2$ substructure is selected such that it matches the one in [21]. The resulting massless spectra for the cases with local RR charge cancellation in the compact space, however, coincide with the old non-chiral $\Omega\mathcal{R} \times \mathbb{Z}_4 \times \mathbb{Z}_2$ models [5] where a different set of matrices was used.

The generic gauge group supported by a stack of N_a identical D6-branes is broken down by the $\mathbb{Z}_2 \times \mathbb{Z}_2$ symmetry from the initial $U(N_a)$ factor to a subgroup $U(N_a/2)$. If the D6-branes are their own mirror images under \mathcal{R} , the gauge group is further reduced to $Sp(N_a/2)$.² On a generic representation of a unitary gauge factor, the antiholomorphic involution \mathcal{R} acts as complex conjugation.

The aa strings provide three chiral multiplets in the adjoint representation of $U(N_a/2)$ which are associated to separating identical D6-branes parallelly by a distance on the three two-tori T_j^2 . The $a(\Theta a)$ sector is supersymmetric as well. It provides a chiral multiplet in the adjoint representation of $U(N_a/2)$ at each intersection point on $T_1^2 \times T_2^2$ which is associated to recombining the brane a and its \mathbb{Z}_4 image (Θa) and moving the recombined brane away from the intersection point [24]. The situation is schematically depicted in figure 4.

For arbitrary choices of wrapping numbers and radii R_1 and R_2 , the remaining sectors aa' , $a(\Theta a)'$, $ab \dots$ are non-supersymmetric. The general chiral spectrum is displayed in table 1. The chiral fermions are accompanied by a bunch of scalar pseudo-superpartners with the same gauge quantum numbers whose masses depend on the six wrapping numbers n_i^a, m_i^a , the radii R_1, R_2 and shape $b = 0, 1/2$ of the third torus T_3^2 .

The four kinds of D6-branes which lie on top of the O6-planes correspond to the so called ‘filler branes’ of the $T^6/(\mathbb{Z}_2 \times \mathbb{Z}_2)$ model in [23] plus their \mathbb{Z}_4 images. They provide for symplectic gauge factors. Their intersections among each other provide only for non-chiral matter and are supersymmetric. Their wrapping numbers are explicitly listed in appendix A, equation (24). The intersections of ‘filler branes’ with arbitrary D6-branes yield the contribution to the chiral spectrum displayed in table 2. The vanishing of the chiral anomaly can be checked by imposing

²We follow the convention where the adjoint representation of $Sp(N_a/2)$ has $\frac{1}{2} \frac{N_a}{2} (\frac{N_a}{2} + 1)$ degrees of freedom.

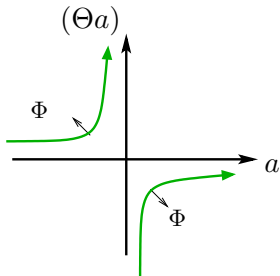


Figure 4: Schematic picture of the recombination of a brane a and its \mathbb{Z}_4 image (Θa) triggered by a supermultiplet Φ in the adjoint representation.

the RR tadpole cancellation conditions (7) bearing in mind that the ‘filler branes’ contribute only half the amount to the tadpole equations since they are their own $\mathcal{R}(\Theta)$ images.

Green Schwarz mechanism

In general, the models provide several $U(1)$ factors. As in the T^6/\mathbb{Z}_3 orbifold model in [12], the Green Schwarz mechanism is mediated by the two-form ${}^{(4)}B_2$ which is obtained by dimensional reduction from the ten dimensional two-form ${}^{(10)}C_2$. The dual four dimensional axion ${}^{(4)}C_0$ is given by ${}^{(4)}C_0 = \int_{T^6} {}^{(10)}C_6$. The three other dual pairs of RR forms present in the toroidal case [11] are projected out by the orbifold symmetry. The coupling of a single $D6_a$ -brane to the RR forms is the same as in the toroidal case [11]. The orbifold symmetry is taken into account by summing over all four D6-branes in the orbit of brane a . The resulting couplings are

$$\begin{aligned} \int_{\mathbb{R}^{1,3}} \sum_a N_a (n_a^1 N_a^2 + m_a^1 M_a^2) M_a^3 B_2 \wedge F_a, \\ \int_{\mathbb{R}^{1,3}} \sum_b (n_b^1 N_b^2 + m_b^1 M_b^2) n_b^3 C_0 \wedge F_b \wedge F_b. \end{aligned} \tag{9}$$

The first equation in (9) can give mass to one $U(1)$ factor, even if it is anomaly-free [11].

Non-chiral states

Non-chiral massless states arise from intersections of D6-branes parallel on at least one two-torus and from intersections of ‘filler branes’ c_i and c_j . These states are listed in table 3. The part of the non-chiral spectrum which involves only ‘filler branes’ is supersymmetric and can easily be seen to be identical to the one computed in [5] for the special case $N_{c_1} = N_{c_2} = N_{c_3} = N_{c_4} = 16/4^b$.

General chiral spectrum		
	multiplicity	representation
aa	$3 + \frac{1}{2}((n_1^a)^2 + (m_1^a)^2)((N_2^a)^2 + (M_2^a)^2)$	$U(N_a/2)$ Adj_a
ab	$I_{ab} + I_{a(\Theta b)}$	$(\mathbf{F}_a, \overline{\mathbf{F}}_b)$
ab'	$I_{ab'} + I_{a(\Theta b)'}$	$(\mathbf{F}_a, \mathbf{F}_b)$
aa'	$\frac{1}{2}(I_{aa'} + I_{a(\Theta a)'})$	Sym_a
	$-\frac{1}{2}(I_{a(\Theta a)\Theta}^{\Omega\mathcal{R}} + I_{a(\Theta a)'}^{\Omega\mathcal{R}\Theta^3} + I_{a(\Theta a)\Theta}^{\Omega\mathcal{R}\Theta\omega} + I_{a(\Theta a)'}^{\Omega\mathcal{R}\Theta^3\omega})$	
	$\frac{1}{2}(I_{aa'} + I_{a(\Theta a)'})$	Anti_a
	$+\frac{1}{2}(I_{a(\Theta a)\Theta}^{\Omega\mathcal{R}} + I_{a(\Theta a)'}^{\Omega\mathcal{R}\Theta^3} + I_{a(\Theta a)\Theta}^{\Omega\mathcal{R}\Theta\omega} + I_{a(\Theta a)'}^{\Omega\mathcal{R}\Theta^3\omega})$	

Table 1: General chiral spectrum for the $T^6/(\Omega\mathcal{R} \times \mathbb{Z}_4 \times \mathbb{Z}_2)$ orientifold. $\mathbf{F}_a = \mathbf{N}_a/2$ denotes the fundamental representation of $U(N_a/2)$. **Adj_a**, **Sym_a** and **Anti_a** denote the adjoint, symmetric and antisymmetric representations. The explicit expressions for the intersection numbers are given in appendix A equation (23).

5 NSNS tadpoles

The computation of NSNS and NSNS $(-1)^F$ contributions to the tadpoles goes along the same lines as the one of the RR tadpoles. One obtains a sum of perfect squares,

$$\left(\sum_a \frac{L_1^a L_2^a L_3^a}{R_A R_B v} - 16\sqrt{2}(u + \frac{1}{4^b} \frac{1}{u}) \right)^2 + \left(\sum_a \frac{L_1^a L_2^a}{R_A R_B v} \frac{(n_3^a R_1)^2 - (M_3^a R_2)^2}{L_3^a} - 16\sqrt{2}(u - \frac{1}{4^b} \frac{1}{u}) \right)^2$$

General chiral spectrum containing ‘filler branes’ c		
	multiplicity	representation
cc	$3 + 2$	$Sp(N_c/2)$ Anti_c
cb	$I_{cb} + I_{c(\Theta b)}$	$(\mathbf{F}_c, \overline{\mathbf{F}}_b)$

Table 2: General contribution to the chiral spectrum for the $T^6/(\Omega\mathcal{R} \times \mathbb{Z}_4 \times \mathbb{Z}_2)$ orientifold from sectors including ‘filler branes’ c and branes b with arbitrary positions. The explicit expressions for the intersection numbers are given in appendix A, equation (25).

Non-chiral spectrum		
	multiplicity	representation
ab	$\prod_{i \neq i_0} I_{ab}^i + \prod_{i \neq i_0} I_{a(\Theta b)}^i$	$(\mathbf{F}_a, \overline{\mathbf{F}}_b) + (\overline{\mathbf{F}}_a, \mathbf{F}_b)$
ab'	$\prod_{i \neq i_0} I_{ab'}^i + \prod_{i \neq i_0} I_{a(\Theta b)'}^i$	$(\mathbf{F}_a, \mathbf{F}_b) + (\overline{\mathbf{F}}_a, \overline{\mathbf{F}}_b)$
ac	$\prod_{i \neq i_0} I_{ac}^i + \prod_{i \neq i_0} I_{a(\Theta c)}^i$	$(\mathbf{F}_a, \mathbf{F}_c) + (\overline{\mathbf{F}}_a, \mathbf{F}_c)$
$c_1 c_2$	$3 \cdot 4^b$	$(\mathbf{F}_{c_1}, \mathbf{F}_{c_2})$
$c_1 c_3$	2	$(\mathbf{F}_{c_1}, \mathbf{F}_{c_3})$
$c_1 c_4$	4^b	$(\mathbf{F}_{c_1}, \mathbf{F}_{c_4})$
$c_2 c_3$	4^b	$(\mathbf{F}_{c_2}, \mathbf{F}_{c_3})$
$c_2 c_4$	2	$(\mathbf{F}_{c_2}, \mathbf{F}_{c_4})$
$c_3 c_4$	$3 \cdot 4^b$	$(\mathbf{F}_{c_3}, \mathbf{F}_{c_4})$

Table 3: Massless non-chiral spectrum for the $T^6/(\Omega\mathcal{R} \times \mathbb{Z}_4 \times \mathbb{Z}_2)$ orientifold with sectors including ‘filler branes’. In addition, representations $(\mathbf{Anti}_a + \overline{\mathbf{Anti}}_a)$ and $(\mathbf{Sym}_a + \overline{\mathbf{Sym}}_a)$ occur at intersection of a with a' and $(\Theta a)'$ if they are parallel on at least one torus.

where $v = \sqrt{R_1 R_2}$ and $u = \sqrt{R_1/R_2}$ are the square roots of the volume and the imaginary part of the complex structure of T_3^2 . Using the notation

$$\mathcal{L}_3^a(u) = \sqrt{(n_3^a u)^2 + \left(\frac{M_3^a}{u}\right)^2}, \quad vu \partial_u \mathcal{L}_3^a(u) = \frac{(n_3^a R_1)^2 - (M_3^a R_2)^2}{L_3^a},$$

the NSNS tadpoles can be rewritten as

$$\left(\sum_a \frac{L_1^a L_2^a \mathcal{L}_3^a}{R_A R_B} - 16\sqrt{2} \left(u + \frac{1}{4^b} \frac{1}{u} \right) \right)^2 + \left(u \partial_u \left[\sum_a \frac{L_1^a L_2^a \mathcal{L}_3^a}{R_A R_B} - 16\sqrt{2} \left(u + \frac{1}{4^b} \frac{1}{u} \right) \right] \right)^2.$$

The term in the first bracket is proportional to the overall volume of the D6-branes minus the volume of the O6-planes and therefore the dilaton tadpole. The term in the second bracket gives the complex structure tadpole for T_3^2 since it is proportional to the derivative with respect to u .

From this identification of the NSNS tadpoles, the scalar potential is deduced to be

$$V(\Phi_s, u) = e^{-\Phi_s} \left(\sum_{a=1}^K N_a \frac{\prod_{i=1}^3 L_a^i}{R_A R_B R_1} - 16\sqrt{2} \left(u + \frac{1}{4^b} \frac{1}{u} \right) \right). \quad (10)$$

Using the relation (26) in appendix B between wrapping numbers and the tangent of the angles φ_i^a with respect to the real axes, the compact volume of a D6_a-brane can in general be rewritten as

$$\left(\prod_{i=1}^3 L_i^a \right)^2 = \left(R_A R_B R_1 n_1^a \frac{N_2^a}{\sqrt{2}} n_3^a \right)^2 \left(\left(1 - \sum_{i=1}^3 \tan \varphi_i^a \tan \varphi_{i+1}^a \right)^2 + \left(\sum_{i=1}^3 \tan \varphi_i^a - \prod_{i=1}^3 \tan \varphi_i^a \right)^2 \right).$$

Since the necessary condition for preserving supersymmetry, $\sum_{i=1}^3 \varphi_i^a = 0$, in terms of the tangents reads

$$\sum_{i=1}^3 \tan \varphi_i^a = \prod_{i=1}^3 \tan \varphi_i^a, \quad (11)$$

it is quite obvious that the scalar potential (10) vanishes iff the whole D6-brane configuration preserves supersymmetry.

6 Chiral supersymmetric models

One of the motivations to study type IIA compactifications on $T^6/(\mathbb{Z}_4 \times \mathbb{Z}_2)$ with intersecting D6-branes consists in the quest for phenomenologically appealing chiral spectra. It turns out to be a difficult task to find general classes of models which satisfy (11) and are free of symmetric representations of a unitary gauge factor. In general, six wrapping numbers per D6-brane orbit are only constrained by these two conditions. The only relevant modulus of the compactification is the ratio of radii R_1/R_2 which is fixed by a single supersymmetric D6-brane orbit at non-trivial angle on T_3^2 together with the discrete quantity $b = 0$ or $1/2$.

In order to start the search systematically, we restrict to the cases where the D6-branes lie on top of an O6-plane on one two-torus. By virtue of supersymmetry, these D6-branes are specified by only one non-trivial angle ϑ . There exist six different orbits of this kind with respect to Θ and \mathcal{R} . Each orbit is characterized by one of the following D6-branes,

$$\begin{aligned} a_1 : \quad & \varphi_1 = 0, \varphi_2 = \vartheta_1, \varphi_3 = -\vartheta_1, \\ a_2 : \quad & \varphi_1 = \vartheta_2, \varphi_2 = 0, \varphi_3 = -\vartheta_2, \\ a_3 : \quad & \varphi_1 = \vartheta_3, \varphi_2 = -\vartheta_3, \varphi_3 = 0, \\ a_4 : \quad & \varphi_1 = \frac{\pi}{4}, \varphi_2 = \vartheta_4, \varphi_3 = -\vartheta_4 - \frac{\pi}{4}, \\ a_5 : \quad & \varphi_1 = \vartheta_5, \varphi_2 = \frac{\pi}{4}, \varphi_3 = -\vartheta_5 - \frac{\pi}{4}, \\ a_6 : \quad & \varphi_1 = \vartheta_6, \varphi_2 = -\vartheta_6 - \frac{\pi}{2}, \varphi_3 = \frac{\pi}{2}. \end{aligned} \quad (12)$$

The corresponding 3-cycles are depicted in figure 5. The necessary conditions for preserving supersymmetry in each case in terms of wrapping numbers are explicitly listed in appendix B, equation (27).

In the cases $a_3 \dots a_6$, the choices of angles $\vartheta_i = 0, \frac{\pi}{4} \pmod{\frac{\pi}{2}}$ correspond to selecting one of the supersymmetric ‘filler branes’ $c_j (j = 1 \dots 4)$, and the D6-brane orbit again contains only two distinct 3-cycles.

In the cases of D6-branes a_1 and a_2 , choosing $\vartheta_i = \frac{\pi}{4}$ leads to a non-trivial supersymmetric configuration. The following identities hold independently of the values of the radii R_1, R_2 and

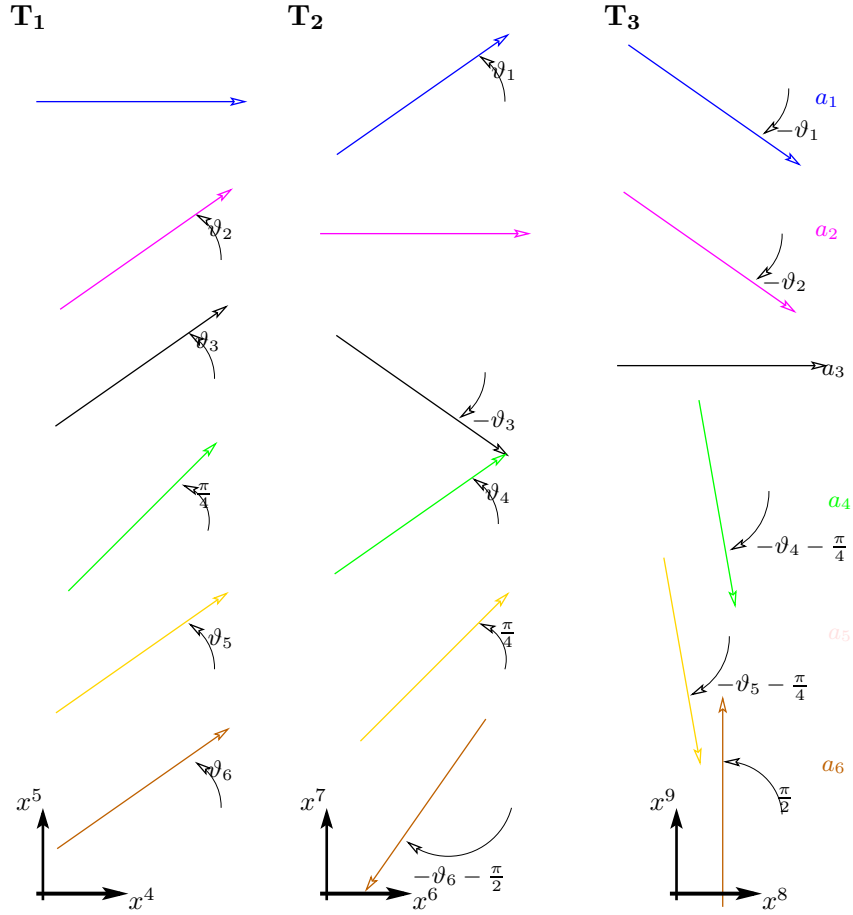


Figure 5: Special supersymmetric D6-brane configurations. Only one representant of each orbit containing four distinct D6-branes is depicted for the sake of clarity. The lattice on $T_1^2 \times T_2^2$ is \mathbf{AB} , T_3^2 can be rectangular or tilted.

b as long as the angles are chosen to be $\vartheta_1 = \vartheta_2 = \frac{\pi}{4}$:

$$\begin{aligned} I_{a_1 a_2} + I_{a_1(\Theta a_2)} &= 0, \\ I_{a_1 a'_2} + I_{a_1(\Theta a_2)'} &= 0, \\ I_{Sym}^{a_1} &= -I_{Anti}^{a_1} = 2n_3^{a_1} \left(-\frac{1}{4^b} + \frac{R_1}{R_2} \right), \\ I_{Sym}^{a_2} &= -I_{Anti}^{a_2} = 4n_3^{a_2} \left(-\frac{1}{4^b} + \frac{R_1}{R_2} \right). \end{aligned}$$

This means that there is no antisymmetric or symmetric representation of a chiral field associated to the stacks a_1 and a_2 , as long as

$$\frac{R_1}{R_2} = \frac{1}{4^b}$$

is fulfilled, which is the condition for obtaining the rectangular **A** and **B** lattice for $b = 0, 1/2$ respectively.

Implementing the constraint $\vartheta_1 = \vartheta_2 = \frac{\pi}{4}$ together with no symmetric representation of the gauge group fixes the wrapping numbers of the first two kinds of special D6-branes completely up to the choice $b = 0, 1/2$ of the lattice T_3^2 ,

$$\begin{aligned} \text{brane:} & \quad (n_1, m_1) \times (N_2, M_2) \times (n_3, M_3) \\ A_1 : & \quad (1, 0) \times (1, -1) \times \left(1, -\frac{1}{4^b}\right), \\ A_2 : & \quad (1, 1) \times (2, 0) \times \left(1, -\frac{1}{4^b}\right). \end{aligned} \tag{13}$$

Constraining the D6-brane set-up now to consist of only these two non-trivial kinds of D6-branes A_1, A_2 and the four kinds of ‘filler branes’ c_j , the tadpole cancellation conditions read

$$32 = N_{A_1} + 2N_{A_2} + 4^b (N_{c_1} + N_{c_3}) = N_{A_1} + 2N_{A_2} + 4^b (N_{c_2} + N_{c_4}).$$

The resulting gauge group of this set-up is $U\left(\frac{N_{A_1}}{2}\right) \times U\left(\frac{N_{A_2}}{2}\right) \times Sp\left(\frac{N_{c_1}}{2}\right) \times Sp\left(\frac{N_{c_2}}{2}\right) \times Sp\left(\frac{N_{c_3}}{2}\right) \times Sp\left(\frac{N_{c_4}}{2}\right)$, and the corresponding chiral spectrum consists only of bifundamental states,

$$\begin{aligned} & 1 \times [(\mathbf{F}_{A_1}, \mathbf{F}_{c_1}) + (\overline{\mathbf{F}}_{A_1}, \mathbf{F}_{c_2}) + (\mathbf{F}_{A_1}, \mathbf{F}_{c_3}) + (\overline{\mathbf{F}}_{A_1}, \mathbf{F}_{c_4})] \\ & + 2 \times [(\mathbf{F}_{A_2}, \mathbf{F}_{c_1}) + (\overline{\mathbf{F}}_{A_2}, \mathbf{F}_{c_2}) + (\mathbf{F}_{A_2}, \mathbf{F}_{c_3}) + (\overline{\mathbf{F}}_{A_2}, \mathbf{F}_{c_4})]. \end{aligned}$$

As already mentioned in section 4, the notation of symplectic gauge factors is such that $\frac{N_{c_j}}{2} \in 2\mathbb{N}$ is required.

A supersymmetric Pati-Salam model with four generations

The general class of models described in the last paragraph can be used to construct explicit semi-realistic chiral spectra. A supersymmetric Pati-Salam model with four generations is obtained by choosing the numbers of identical D6-branes to be $N_{A_2} = 8$, $N_{c_1} = N_{c_2} = N_{c_3} = N_{c_4} = 4$ and the tilted torus, i.e. $b = 1/2$. The resulting gauge group is

$$U(4) \times Sp(2)^4 \tag{14}$$

with the chiral matter content

$$2 \times [(\mathbf{4}, \mathbf{2}_1) + (\bar{\mathbf{4}}, \mathbf{2}_2) + (\mathbf{4}, \mathbf{2}_3) + (\bar{\mathbf{4}}, \mathbf{2}_4)]. \quad (15)$$

In this case, since $Sp(2) \simeq SU(2)$, the gauge group $U(4) \times SU(2)_L \times SU(2)_R$ is obtained by identifying $SU(2)_1 \simeq SU(2)_3$ and $SU(2)_2 \simeq SU(2)_4$ via brane recombination. The required kind of Higgs effect is commented on below. The unitary factor $U(4)$ is, furthermore, broken down to $U(3) \times U(1)$ by separating the stack of branes A_2 at least on one two-torus, e.g. on T_3^2 , into two parallel sets with $N_{A_2}^{(1)} = 6$, $N_{A_2}^{(2)} = 2$. In the T-dual type IIB orientifold, the breaking of the gauge group is triggered by a Wilson line on the corresponding two-torus. From a field theoretic point of view, the three adjoint fields originating from the aa sector parameterize the brane positions on the three two-tori T_j^2 . A suitable vev. for one of the adjoint scalars leads to the required breaking of the gauge group. This mechanism can always occur, since these adjoint scalars are flat directions of the compactification.

Out of the two $U(1)$ factors which emerge from the decomposition $U(4) \rightarrow U(3) \times U(1)_2 \rightarrow SU(3) \times U(1)_1 \times U(1)_2$ in this model, the linear combination

$$U(1)_{B-L} = \frac{1}{3}(U(1)_1 - 3U(1)_2) \quad (16)$$

is massless and anomaly-free. The quantum numbers of the chiral fields under $U(1)_{B-L}$ are the correct ones for a model containing right handed neutrinos. The second $U(1)$ factor is also anomaly-free, but acquires a mass through the Green Schwarz mechanism in equation (9).

A supersymmetric Pati-Salam model with three generations

Starting again with the set of D6-branes $A_1, A_2, c_1, c_2, c_3, c_4$, it is possible to construct models with three generations but two $U(4)$ factors. More concretely, the choice $N_{A_1} = N_{A_2} = 8$, $N_{c_1} = N_{c_2} = 4$ with $b = 1/2$ leads to a left-right symmetric Pati - Salam model with initial gauge group

$$U(4)_1 \times U(4)_2 \times Sp(2)_1 \times Sp(2)_2 \quad (17)$$

and chiral spectrum

$$1 \times [(\mathbf{4}_1, \mathbf{2}_1) + (\bar{\mathbf{4}}_1, \mathbf{2}_2)] + 2 \times [(\mathbf{4}_2, \mathbf{2}_1) + (\bar{\mathbf{4}}_2, \mathbf{2}_2)]. \quad (18)$$

Brane recombination of A_1 and A_2 into a single non-factorizable brane and the isomorphism $Sp(2)_1 \simeq SU(2)_L$, $Sp(2)_2 \simeq SU(2)_R$ lead to the usual Pati - Salam group $U(4) \times SU(2)_L \times SU(2)_R$ with three generations of chiral matter $3 \times [(\mathbf{4}, \mathbf{2}_L) + (\bar{\mathbf{4}}, \mathbf{2}_R)]$.

The discussion of Abelian symmetries is identical to the one for the four generation model, i.e. a separation on T_3^2 of the stacks A_1, A_2 into parallel sets $N_{A_1}^{(1)} = N_{A_2}^{(1)} = 6$, $N_{A_1}^{(2)} = N_{A_2}^{(2)} = 2$ leads to the desired gauge symmetry breaking $U(4) \rightarrow SU(3) \times U(1)_{B-L}$ after brane recombination.

Brane recombination

In the model under consideration with three generations, the two kinds of branes A_1, A_2 which are supposed to recombine into a single non-factorizable brane preserve a common $\mathcal{N} = 2$ supersymmetry since they are parallel on the third two-torus T_3^2 . In general, a brane recombination will take place if the volume of the complex cycle wrapped by the non-factorizable brane is

smaller than the the sum of the volumina of the factorizable cycles. On the other hand, since the original configuration is supersymmetric in this case, the volume of the final brane configuration will be the same as the initial one and the configuration is marginally stable.

The D-term potential for an $U(M_a) \times U(M_b)$ gauge symmetry with $M_a = M_b$ and $\mathcal{N} = 2$ hypermultiplets whose complex scalar components are denoted by H_1^i, H_2^i in the bifundamental representations $(\mathbf{F}_a, \overline{\mathbf{F}}_b)$ and $(\overline{\mathbf{F}}_a, \mathbf{F}_b)$, respectively, vanishes provided that the following equations are fulfilled,

$$\begin{aligned} \sum_i (H_1^i T_G^a (H_1^i)^\dagger - (H_2^i)^\dagger T_G^a H_2^i) &= 0, \\ \sum_i ((H_1^i)^\dagger T_G^b H_1^i - H_2^i T_G^b (H_2^i)^\dagger) &= 0. \end{aligned} \tag{19}$$

$i = 1 \dots I_{ab} + I_{a(\Theta b)}$ labels the number of hypermultiplets which is in the intersecting D6-brane models given by the number of brane intersections. T_G^a and T_G^b label the generators of the gauge factors $U(M_a)$ and $U(M_b)$, respectively. The gauge indices are summed in such a way that e.g. in the first row in (19), the index of H_1^i pertaining to the first gauge factor $U(M_a)$ is contracted with the generator T_G^a etc. Imposing vev.s of the scalars in the hypermultiplets to be proportional to the identity matrix, i.e. $\langle H_j^i \rangle = h_j^i \mathbb{1}$ ($j = 1, 2$), reduces the D-term potential to its $U(1)$ part [24]

$$V_D = \frac{1}{2g^2} \left(\sum_i h_1^i \bar{h}_1^i - \sum_i h_2^i \bar{h}_2^i \right)^2. \tag{20}$$

The superpotential contributes to the F-terms via

$$W = \sum_i (H_1^i \Phi_a H_2^i - H_1^i \Phi_b H_2^i) \tag{21}$$

where Φ_a, Φ_b are fields in the adjoint representation of the respective gauge factors and contraction of all gauge indices is understood. Imposing diagonal vev.s as above reduces the requirement of vanishing F-term contributions to the potential to

$$\sum_i h_1^i h_2^i = 0. \tag{22}$$

Therefore, a flat direction admitting brane recombination occurs in the presence of at least two hypermultiplets, e.g. for $h_1^1 = h_2^2 = h \neq 0, h_1^2 = h_2^1 = 0$. This is exactly the case for the three generation model with initial gauge group $U(4)_1 \times U(4)_2$ where one hypermultiplet is provided by the intersection of A_1 with A_2 and the other one by the intersection of A_1 with (ΘA_2) . A generic value for h provides the required recombination of A_1 and A_2 including their respective \mathbb{Z}_4 images into a single non-factorizable brane with gauge group $U(4)$.

In the model with four generations, brane recombination is supposed to occur among the $Sp(2)$ factors. The discussion of D-terms in this case is similar to the previous one regarding the $Sp(2)$ factors as $SU(2)$ s. However, due to the absence of an Abelian factor, the D-terms vanish identically for vev.s proportional to the identity. From table 3, one can read off that there exist always two chiral multiplets in the required bifundamental representation of the symplectic gauge factors at the intersections $c_1 c_3 + c_1(\Theta c_3)$ and $c_2 c_4 + c_2(\Theta c_4)$. These bifundamentals are expected to trigger the brane recombination processes $c_1 + c_3 \rightarrow c_L, c_2 + c_4 \rightarrow c_R$ which lead to the final gauge group $U(4) \times SU(2)_L \times SU(2)_R$. A more precise description of this process

would, however, require a more detailed analysis of the F-terms in this $\mathcal{N} = 1$ supersymmetric sector.

As mentioned in [15], the $SU(2)_R$ symmetry in both models might also be broken down to a $U(1)$ factor by parallelly displacing the brane c_2 in the three generation model and $c_2 + c_4 = c_R$ in the four generation model from the O6-planes, e.g. on the third two-torus T_3^2 , in such a way that the whole configuration again respects the $\Omega\mathcal{R}$ symmetry.

7 Conclusions

In this paper, a type IIA orientifold in the orbifold background $T^6/(\mathbb{Z}_4 \times \mathbb{Z}_2)$ with intersecting D6-branes has been studied. The RR tadpole cancellation conditions and the scalar potential at disc level have been computed. The general chiral spectrum has been derived, the non-chiral part of the low energy spectrum has been considered and two examples of supersymmetric models with a Pati-Salam gauge group have been given, thus proving that it is worthwhile to consider this orientifold model in greater detail. In particular, the first supersymmetric and stable three generation model with right handed fermions but no further exotic chiral matter has been found whereas all previous chiral supersymmetric models from intersecting D6-branes on $T^6/(\mathbb{Z}_2 \times \mathbb{Z}_2)$ and T^6/\mathbb{Z}_4 contained some exotic matter. As in the latter models, the complex structure moduli on two of the three two-tori are frozen by the $\mathbb{Z}_4 \times \mathbb{Z}_2$ symmetry whereas no such constraint arises in the $T^6/(\mathbb{Z}_2 \times \mathbb{Z}_2)$ case.

However, many open questions remain. On the one hand, it is worthwhile to search more systematically for (supersymmetric) models with exactly the chiral MSSM content as well as GUT generalizations. Furthermore, the non-chiral sectors need to be studied in full detail in order to understand the exact mechanisms of gauge- and supersymmetry breaking and brane recombination as well as the low energy features of these models. Phenomenological aspects of these models including the computation of gauge couplings similar to those in [22] for the $T^6/(\mathbb{Z}_2 \times \mathbb{Z}_2)$ orbifold and Yukawa couplings as computed in [15] for the toroidal case also deserve further study. Furthermore, the gauge threshold corrections as recently considered for intersecting D6-branes in [27] deserve to be worked out in detail for the model presented in this article. However, it has to be taken into account that in these two specific models, recombined branes wrap non-factorizable cycles and thus a generalization of all phenomenological quantities explicitly derived for factorizable branes is required.

Last but not least, in order to understand M-theory better, it is an interesting issue to explore in more detail the type II and heterotic dual models.

Acknowledgments

It am grateful to D. Cremades, L. Ibáñez, F. Marchesano and A. Uranga for helpful discussions and comments. Furthermore, I wish to thank K. Wendland for the computation of the Hodge numbers in this orbifold model.

This work is supported by the RTN program under contract number HPRN-CT-2000-00148.

A Intersection numbers

The explicit expressions for the intersection numbers of the orbits of brane a with brane b in term of the wrapping numbers are

$$\begin{aligned}
I_{ab} + I_{a(\Theta b)} &= \frac{1}{2}(n_1^a m_1^b - m_1^a n_1^b)(N_2^a M_2^b - M_2^a N_2^b)(-n_3^a M_3^b + M_3^a n_3^b) \\
&\quad + \frac{1}{2}(n_1^a n_1^b + m_1^a m_1^b)(N_2^a N_2^b + M_2^a M_2^b)(-n_3^a M_3^b + M_3^a n_3^b), \\
I_{ab'} + I_{a(\Theta b)'} &= \frac{1}{2}(n_1^a m_1^b + m_1^a n_1^b)(N_2^a M_2^b + M_2^a N_2^b)(n_3^a M_3^b + M_3^a n_3^b) \\
&\quad - \frac{1}{2}(n_1^a n_1^b - m_1^a m_1^b)(-N_2^a N_2^b + M_2^a M_2^b)(n_3^a M_3^b + M_3^a n_3^b), \\
I_{Sym}^a &= \frac{1}{2}(I_{aa'} + I_{a(\Theta a)'}) \\
-\frac{1}{2}(I_{a(\Theta a)'}^{\Omega \mathcal{R} \Theta} + I_{a(\Theta a)'}^{\Omega \mathcal{R} \Theta^3} + I_{a(\Theta a)'}^{\Omega \mathcal{R} \Theta \omega} + I_{a(\Theta a)'}^{\Omega \mathcal{R} \Theta^3 \omega}) &= -\frac{2}{4^b}(m_1^a N_2^a - n_1^a M_2^a)n_3^a - 2(m_1^a M_2^a + n_1^a N_2^a)M_3^a \\
&\quad + 2m_1^a n_1^a M_2^a N_2^a n_3^a M_3^a \\
&\quad + \frac{1}{2}((n_1^a)^2 - (m_1^a)^2)((N_2^a)^2 - (M_2^a)^2)n_3^a M_3^a, \\
I_{Anti}^a &= \frac{1}{2}(I_{aa'} + I_{a(\Theta a)'}) \\
+\frac{1}{2}(I_{a(\Theta a)'}^{\Omega \mathcal{R} \Theta} + I_{a(\Theta a)'}^{\Omega \mathcal{R} \Theta^3} + I_{a(\Theta a)'}^{\Omega \mathcal{R} \Theta \omega} + I_{a(\Theta a)'}^{\Omega \mathcal{R} \Theta^3 \omega}) &= \frac{2}{4^b}(m_1^a N_2^a - n_1^a M_2^a)n_3^a + 2(m_1^a M_2^a + n_1^a N_2^a)M_3^a \\
&\quad + 2m_1^a n_1^a M_2^a N_2^a n_3^a M_3^a \\
&\quad + \frac{1}{2}((n_1^a)^2 - (m_1^a)^2)((N_2^a)^2 - (M_2^a)^2)n_3^a M_3^a,
\end{aligned} \tag{23}$$

where the abbreviations (5) have been used.

The wrapping numbers of the $\mathcal{R}\Theta^k$ invariant ‘filler branes’ are

$$\begin{aligned}
\text{brane:} &\quad (n_1, m_1) \times (N_2, M_2) \times (n_3, M_3) \\
c_1 : &\quad (1, 0) \times (2, 0) \times (4^b, 0), \\
c_2 : &\quad (1, 0) \times (0, -2) \times (0, -1), \\
c_3 : &\quad (1, 1) \times (1, 1) \times (4^b, 0), \\
c_4 : &\quad (1, 1) \times (1, -1) \times (0, -1).
\end{aligned} \tag{24}$$

For intersections of ‘filler branes’ c with arbitrary branes b , the intersection numbers are given by

$$I_{cb} + I_{c(\Theta b)} = \begin{cases} -4^b(n_1^b N_2^b + m_1^b M_2^b)M_3^b & M_3^c = 0, \\ -(m_1^b N_2^b - n_1^b M_2^b)n_3^b & M_3^c = -1. \end{cases} \tag{25}$$

B Supersymmetry conditions on intersection numbers

The angles on the three two-tori with respect to the real axes in terms of the wrapping numbers, radii and shape of T_3^2 are given by

$$\begin{aligned}\tan \varphi_1^a &= \frac{m_1^a}{n_1^a}, \\ \tan \varphi_2^a &= \frac{m_2^a - n_2^a}{m_2^a + n_2^a} = -\frac{M_2^a}{N_2^a}, \\ \tan \varphi_3^a &= \frac{(m_3^a + bn_3^a)R_2}{n_3^a R_1} = \frac{M_3^a R_2}{n_3^a R_1}.\end{aligned}\tag{26}$$

Using the relations (26), the supersymmetry conditions (12) for the specific D6-branes characterized by one non-trivial angle ϑ only can be rephrased in terms of wrapping numbers as follows:

$$\begin{aligned}a_1 : \quad & (n_1, m_1) = (1, 0), \quad M_2 = \frac{M_3 R_2}{n_3 R_1} N_2, \\ a_2 : \quad & (N_2, M_2) = (2, 0), \quad m_1 = -\frac{M_3 R_2}{n_3 R_1} n_1, \\ a_3 : \quad & (n_3, M_3) = (4^b, 0), \quad m_1 = \frac{M_2}{N_2} n_1, \\ a_4 : \quad & (n_1, m_1) = (1, 1), \quad M_2 = \frac{n_3 R_1 + M_3 R_2}{n_3 R_1 - M_3 R_2} N_2, \\ a_5 : \quad & (N_2, M_2) = (1, -1), \quad m_1 = -\frac{n_3 R_1 + M_3 R_2}{n_3 R_1 - M_3 R_2} n_1, \\ a_6 : \quad & (n_3, M_3) = (0, -1), \quad m_1 = -\frac{N_2}{M_2} n_1.\end{aligned}\tag{27}$$

The conditions in terms of the wrapping numbers are only necessary conditions. The correct orientation of the D6-branes has to be checked separately.

References

- [1] C. Angelantonj, M. Bianchi, G. Pradisi, A. Sagnotti and Y. S. Stanev, Phys. Lett. B **385** (1996) 96 hep-th/9606169. M. Berkooz and R. G. Leigh, Nucl. Phys. B **483** (1997) 187 hep-th/9605049. Z. Kakushadze and G. Shiu, Phys. Rev. D **56** (1997) 3686 hep-th/9705163. Nucl. Phys. B **520** (1998) 75 hep-th/9706051. Z. Kakushadze, Nucl. Phys. B **512** (1998) 221 hep-th/9704059. Z. Kakushadze, G. Shiu and S. H. Tye, Nucl. Phys. B **533** (1998) 25 hep-th/9804092. G. Zwart, Nucl. Phys. B **526** (1998) 378 hep-th/9708040. D. O’Driscoll, hep-th/9801114. G. Shiu and S. H. Tye, Phys. Rev. D **58** (1998) 106007 hep-th/9805157. J. Lykken, E. Poppitz and S. P. Trivedi, Nucl. Phys. B **543** (1999) 105 hep-th/9806080. G. Aldazabal, A. Font, L. E. Ibáñez and G. Violero, Nucl. Phys. B **536** (1998) 29 hep-th/9804026. J. Park, R. Rabadán and A. M. Uranga, Nucl. Phys. B **570** (2000) 3 hep-th/9907074. M. Cvetič, M. Plumacher and J. Wang, JHEP **0004** (2000) 004 hep-th/9911021. M. Cvetič, A. M. Uranga and J. Wang, Nucl. Phys. B **595** (2001) 63 hep-th/0010091. G. Aldazabal, L. E. Ibáñez, F. Quevedo and A. M. Uranga, JHEP **0008** (2000) 002 hep-th/0005067.

- [2] M. Klein and R. Rabadán, JHEP **0010** (2000) 049 [hep-th/0008173](#).
- [3] M. Berkooz, M. R. Douglas and R. G. Leigh, Nucl. Phys. B **480** (1996) 265 [hep-th/9606139](#).
- [4] R. Blumenhagen, L. Görlich and B. Körs, Nucl. Phys. B **569** (2000) 209 [hep-th/9908130](#).
JHEP **0001** (2000) 040 [hep-th/9912204](#). [hep-th/0002146](#).
- [5] S. Förste, G. Honecker and R. Schreyer, Nucl. Phys. B **593** (2001) 127 [hep-th/0008250](#).
- [6] R. Blumenhagen, L. Görlich, B. Körs and D. Lüst, Nucl. Phys. B **582** (2000) 44
[hep-th/0003024](#). JHEP **0010** (2000) 006 [hep-th/0007024](#). Fortsch. Phys. **49** (2001) 591
[hep-th/0010198](#).
- [7] R. Blumenhagen, B. Körs and D. Lüst, JHEP **0102** (2001) 030 [hep-th/0012156](#).
- [8] G. Aldazabal, S. Franco, L. E. Ibáñez, R. Rabadán and A. M. Uranga, JHEP **0102** (2001)
047 [hep-ph/0011132](#). J. Math. Phys. **42** (2001) 3103 [hep-th/0011073](#).
- [9] C. Bachas, [hep-th/9503030](#).
- [10] C. Angelantonj, I. Antoniadis, E. Dudas and A. Sagnotti, Phys. Lett. B **489** (2000)
223 [hep-th/0007090](#). C. Angelantonj and A. Sagnotti, [hep-th/0010279](#). G. Pradisi,
[hep-th/0210088](#). C. Angelantonj, [hep-th/0212066](#). M. Larosa, [hep-th/0212109](#).
- [11] L. E. Ibáñez, F. Marchesano and R. Rabadán, JHEP **0111** (2001) 002 [hep-th/0105155](#).
L. E. Ibáñez, [hep-ph/0109082](#).
- [12] R. Blumenhagen, B. Körs, D. Lüst and T. Ott, Nucl. Phys. B **616** (2001) 3 [hep-th/0107138](#).
- [13] C. Kokorelis, JHEP **0208** (2002) 018 [hep-th/0203187](#). JHEP **0209** (2002) 029
[hep-th/0205147](#). JHEP **0208** (2002) 036 [hep-th/0206108](#). [hep-th/0207234](#). JHEP
0211 (2002) 027 [hep-th/0209202](#). [hep-th/0210004](#). [hep-th/0210200](#). [hep-th/0211091](#).
[hep-th/0212281](#). S. Förste, G. Honecker and R. Schreyer, JHEP **0106** (2001) 004
[hep-th/0105208](#). J. R. Ellis, P. Kanti and D. V. Nanopoulos, Nucl. Phys. B **647** (2002)
235 [hep-th/0206087](#).
- [14] D. Cremades, L. E. Ibáñez and F. Marchesano, JHEP **0207** (2002) 009 [hep-th/0201205](#).
JHEP **0207** (2002) 022 [hep-th/0203160](#). [hep-ph/0212048](#). [hep-ph/0212064](#). D. M. Ghi-
lencea, L. E. Ibáñez, N. Irges and F. Quevedo, JHEP **0208** (2002) 016 [hep-ph/0205083](#).
D. M. Ghilencea, Nucl. Phys. B **648** (2003) 215 [hep-ph/0208205](#). [hep-ph/0212120](#).
A. M. Uranga, [hep-th/0301032](#).
- [15] D. Cremades, L. E. Ibáñez and F. Marchesano, [hep-th/0302105](#).
- [16] N. Arkani-Hamed, S. Dimopoulos and G. R. Dvali, Phys. Lett. B **429** (1998) 263
[hep-ph/9803315](#). I. Antoniadis, N. Arkani-Hamed, S. Dimopoulos and G. R. Dvali, Phys.
Lett. B **436** (1998) 257 [hep-ph/9804398](#).

- [17] D. Bailin, G. V. Kraniotis and A. Love, Phys. Lett. B **530** (2002) 202 [hep-th/0108131](#). Phys. Lett. B **547** (2002) 43 [hep-th/0208103](#). Phys. Lett. B **553** (2003) 79 [hep-th/0210219](#). [hep-th/0212112](#). G. Honecker, Fortsch. Phys. **50** (2002) 896 [hep-th/0112174](#). JHEP **0201** (2002) 025 [hep-th/0201037](#). D. Cremades, L. E. Ibáñez and F. Marchesano, Nucl. Phys. B **643** (2002) 93 [hep-th/0205074](#).
- [18] R. Blumenhagen, B. Körs and D. Lüst, Phys. Lett. B **532** (2002) 141 [hep-th/0202024](#).
- [19] J. Garcia-Bellido, R. Rabadán and F. Zamora, JHEP **0201** (2002) 036 [hep-th/0112147](#). R. Blumenhagen, B. Körs, D. Lüst and T. Ott, Nucl. Phys. B **641** (2002) 235 [hep-th/0202124](#). N. Jones, H. Stoica and S. H. Tye, JHEP **0207** (2002) 051 [hep-th/0203163](#). M. Gomez-Reino and I. Zavala, JHEP **0209** (2002) 020 [hep-th/0207278](#).
- [20] R. Blumenhagen, V. Braun, B. Körs and D. Lüst, JHEP **0207** (2002) 026 [hep-th/0206038](#). [hep-th/0210083](#). A. M. Uranga, JHEP **0212** (2002) 058 [hep-th/0208014](#).
- [21] M. Cvetič, G. Shiu and A. M. Uranga, Phys. Rev. Lett. **87** (2001) 201801 [hep-th/0107143](#). Nucl. Phys. B **615** (2001) 3 [hep-th/0107166](#). [hep-th/0111179](#).
- [22] M. Cvetič, P. Langacker and G. Shiu, Phys. Rev. D **66** (2002) 066004 [hep-ph/0205252](#). Nucl. Phys. B **642** (2002) 139 [hep-th/0206115](#).
- [23] M. Cvetič, I. Papadimitriou and G. Shiu, [hep-th/0212177](#).
- [24] R. Blumenhagen, L. Görlich and T. Ott, JHEP **0301** (2003) 021 [hep-th/0211059](#).
- [25] A. M. Uranga, [hep-th/0204079](#).
- [26] A. M. Uranga, JHEP **0204** (2002) 016 [hep-th/0201221](#).
- [27] D. Lüst and S. Stieberger, [hep-th/0302221](#).